

*Dušan Arsić*  
*Vukić Lazić*  
*Aleksandar Sedmak*  
*Srbislav Aleksandrović*  
*Jelena Živković*  
*Milan Djordjević*  
*Goran Mladenović*

<https://doi.org/10.21278/TOF.44207>  
ISSN 1333-1124  
eISSN 1849-1391

## **EFFECT OF ELEVATED TEMPERATURES ON MECHANICAL PROPERTIES OF ULTRA HIGH STRENGTH HOT WORK TOOL STEEL H11**

### **Summary**

This paper presents an experimental and numerical study into the influence of elevated temperatures on mechanical properties of the heat treated high quality hot work tool steel H11. This steel belongs to a group of alloyed steels with extraordinary mechanical properties. The aim of this study was to determine the highest temperature at which these properties are still maintained. The experimental investigation focused on the tensile testing of specimens at seven different temperatures, including the room temperature. The highest testing temperature was 700 °C. The heat treatment of plates (specimens) consisted of quenching and tempering. Although the strain hardening of this type of materials is small, the strain hardening curves were calculated to show if there was a possibility for the material to increase its strength due to exploitation loads. Also, a numerical analysis of the tensile test by using the finite element method was done in order to define an appropriate model for numerical testing. The obtained results are then compared with the experimental results.

*Key words:* H11 steel, elevated temperatures, tensile test, strain hardening, FEM

### **1. Introduction**

With constant advancements in mechanical engineering, there is a growing demand for high strength tool steels which could be able to endure a high level of stresses and still be reliable in exploitation. The high quality steel H11 (designation by AISI, by EN-X37CrMoV5-1 and by DIN-X38CrMoV5-1), analyzed in previous investigations by this group of authors [1-4], is used for manufacturing tools, mostly for hot forging and extrusion. During the exploitation, such tools endure extreme pressures which leads to high wear and thermal fatigue. Besides that, the tool material has to deal with high temperature shocks with each stroke of the tool. The forging process is mostly done at high temperatures, thus in order to reduce the influence of high temperatures of the forged piece material, the tool material is preheated to temperatures

between 250 °C and 300 °C. In that way, the gradient of temperatures between the workpiece material and the tool material is lower. However, the pressures to which the tool material is exposed are still very high, which results in the trend to select the highest quality material possible for the manufacture of such tools. Such materials must possess high consistency at elevated temperatures, primarily of tensile properties and resistance to crack initiation [5-10]. This was the reason that led to setting the objective of this study, which is the influence of temperature increase on mechanical properties of the considered steel as well as the ultimate temperature to which the steel could be heated without jeopardizing the tool integrity during forging. The tool life is also an element that affects the quality of forgings as too high and intensive wear/damage of dies and stamps causes a change in the geometry of a manufactured product as well as surface faults (cracks, defects) that are present on a forged product. Similar problems were dealt with by authors [11-13], who were looking for possibilities of applying various methods with the purpose of increasing the life of forging tools. They discovered that compressive stresses greater than 1,000 MPa as well as temperatures of about 800 °C appear on the tool surface, and they presented methods for solving many problems related to the short tool life. Paper [14] presents an analysis of the effect of loading cycles on the behaviour of the AISI H11 tool steel, commonly used for aluminum extrusion dies working at high temperatures and under high stresses. The tests were performed on a Gleeble thermomechanical simulator by heating the specimen using Joule's effect and by applying loading for up to 6.30 h or until the specimen failed. Displacements during the tests at 380, 490, 540 and 580 °C and under the average stresses of 400, 600 and 800 MPa were determined. The results showed that the test could physically simulate the cyclic loading on a hollow die during extrusion and that the creep condition represented the most severe working condition. In addition, the tests could reveal the interaction between creep and fatigue mechanisms. Authors of the paper [15] also analysed the thermal fatigue of tools made of this steel in the temperature range from 100 °C to 650 °C. They recorded stress amplitudes, plastic strain amplitudes and mean stresses in terms of the number of loading cycles. On the other hand, it is interesting to become familiar with the behaviour of this steel during crack initiation and propagation, which is also the research subject [5, 6].

The objective of this study is to show the influence of elevated temperatures on tensile characteristics of the H11 steel and to determine the maximum temperature at which the steel still possesses acceptable properties. Tests were conducted on cylindrical samples on a tensile testing machine which was equipped with a special heating chamber.

## 2. Properties of the tested material, heat treatment of plates and preparation of samples

For the preparation of the specimens the H11 steel was used in the form of a 15 mm thick plate. The chemical composition and mechanical properties are given in Tables 1 and 2.

**Table 1** Chemical composition of steel H11

Designation by AISI	Chemical composition, %							
	C	Si	Mn	P	S	Cr	Mo	V
H11	0.37	1.0	0.4	max 0.03	max 0.02	5.2	1.3	0.4

**Table 2** Mechanical properties of steel H11 at room temperature

Designation by AISI	Soft annealing				Tempering			
	<i>t</i> , °C	HV <sub>max</sub>	<i>R<sub>m</sub></i> , MPa	<i>E</i> , MPa	<i>t</i> , °C	HRC	<i>R<sub>m</sub></i> , MPa	<i>E</i> , MPa
H11	800-830	250	850	≈ 216000	550-660	30-50	1400-1700	≈ 219000

During hot forging or die casting, a number of damage mechanisms act simultaneously to cause cumulative damage to the tool and growing deviations from the original tool

geometry due to wear, micro-chipping, thermal-cracking or breakage. So, it is crucial to determine the optimal heat treatment regime [16, 17]. The prepared plate was heat treated according to the proposed regime. The heat treatment technology assumed quenching and tempering at specific temperatures in order to obtain certain mechanical properties and structure, i.e. the same as properties of forging tools in the production process. The heat treatment regime was as follows (Figure 1a):

- heating up to 1,040 °C, holding on that temperature for 1 hour and then quenching in oil cooled to room temperature. The obtained hardness was approximately 55 HRC.
- double tempering; first at 560 °C, holding for 2 hours and then taking the samples out of the furnace and cool in the air; after the first phase with single-tempered samples is completed, repeating the first tempering cycle.

The SEM micrograph of the tested steel is shown in Figure 1b. The SEM specimen was made from the same plate that was used for the preparation of the tensile specimens. It can be noticed that the whole specimen consists of tempered lath martensite. Tempered martensite is the expected microstructure for this class of steels since that structure has a high resistance to initiation and propagation of cracks and at the same time it exhibits high hardness. Also, no inclusions or defects which could affect the test results were detected in the structure. Defects usually have phosphorus or sulfur origin or there can be carbide particles, which, when grouped or having become larger, can have a significant impact on tensile properties of steel. This is especially the case when defects are larger than 0.1 mm [18].

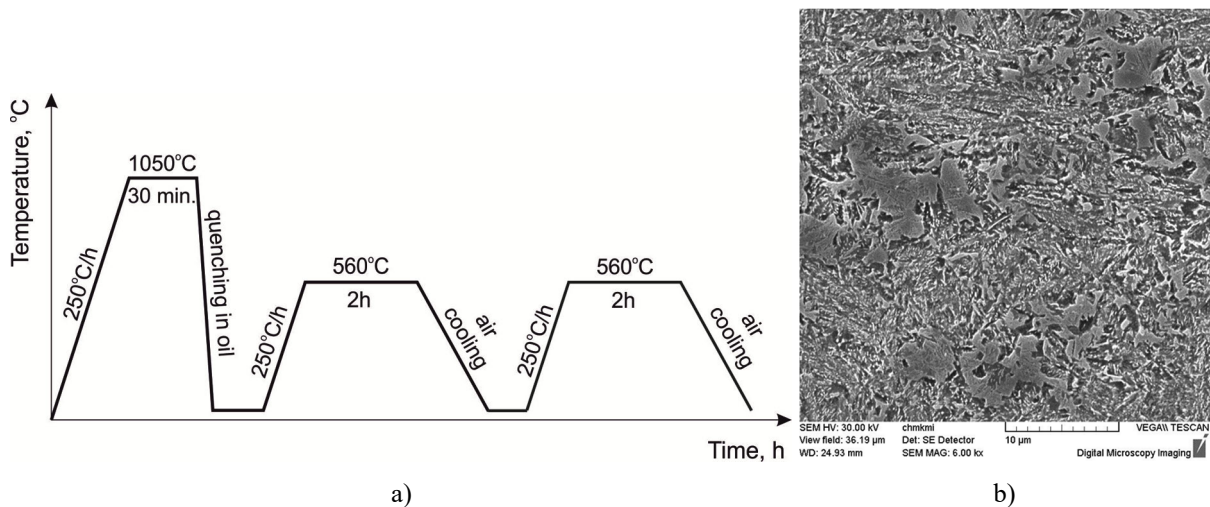


Fig. 1 Heat tretment cycle (a) and specimen microstructure (b)

After the heat treatment, the hardness measurement showed that hardness was about 45-48 HRC, which values were expected. In fact, hardness levels under 45 HRC are rarely used. According to some steel producers [19], for that level of hardness the expected tensile strength at room temperature is  $R_m \approx 1800$  MPa. The samples were prepared by applying turning with a diamond cutting tool and grinding. During the preparation of the samples many problems occur due to the high hardness of the base metal. Although there were even cutting area temperatures reaching up to 600 °C during the processing, hardness did not decrease and the steel maintained high strength [20]. Two specimens and another one as a spare specimen were prepared for each temperature. In the case when the obtained results were approximate, their mean value was shown. On the other hand, when some result deviated from what was expected, the spare specimen was tested to check the experiment. It should be pointed out that tempering temperature has a great influence on fracture surface morphology after tensile testing [21].

The specimens were cylindrical and were prepared according to appropriate standards [22]. A drawing of the specimen and one prepared real specimen are shown in Figure 2. The experimental determination of mechanical properties at elevated temperatures was performed on a universal testing machine Zwick Roell Z100 equipped with a special furnace for specimen heating (Figure 3). Two test specimens were prepared for each testing temperature. The tests were conducted at 20 °C, 300 °C, 400 °C, 500 °C, 600 °C, 650 °C, and at 700 °C.

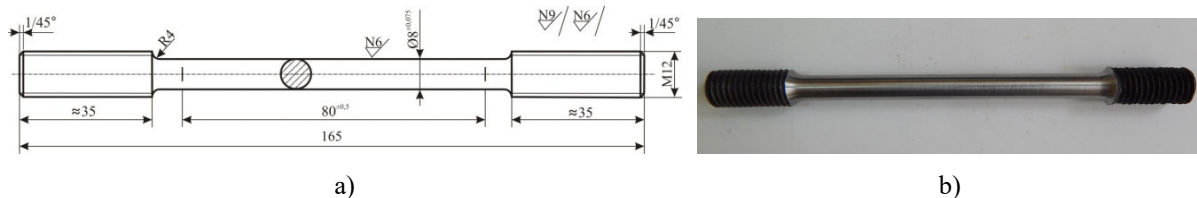


Fig. 2 Tensile testing sample: drawing (a) and real sample (b)



Fig. 3 Testing machine (a) and unit for control of testing temperature (b)

For heating the samples before and during the testing, a MAYTEC heating chamber and a control unit were used. Heating was done by electric spiral heaters positioned on the internal circumference of the chamber. Heaters are positioned along the whole length of the chamber. The temperature was measured by thermocouples positioned in three locations in the chamber – at the bottom, in the middle and on the top of the chamber. The specimens were heated for 30 minutes each to achieve the required temperature across the whole specimen.

### 3. Experimental results

The obtained experimental results are shown in Table 3 and in Figure 4.

Table 3 Experimental results obtained by tensile testing

Steel (AISI)	Sample No.	Testing temperature, °C	Yield stress, $R_{p0.2}$ , MPa	Tensile strength, $R_m$ , MPa	Elongation at maximum force, $A_m$ , %	Elongation at fracture, $A$ , %
H11	1	20	1574	1806	1.62	1.85
	2	300	1370	1550	1.22	1.22
	3	400	1300	1497	1.52	1.57
	4	500	1155	1344	1.33	1.42
	5	600	909	1081	1.61	2.7
	6	650	614	756	1.51	4.1
	7	700	312	396	2.20	20.2

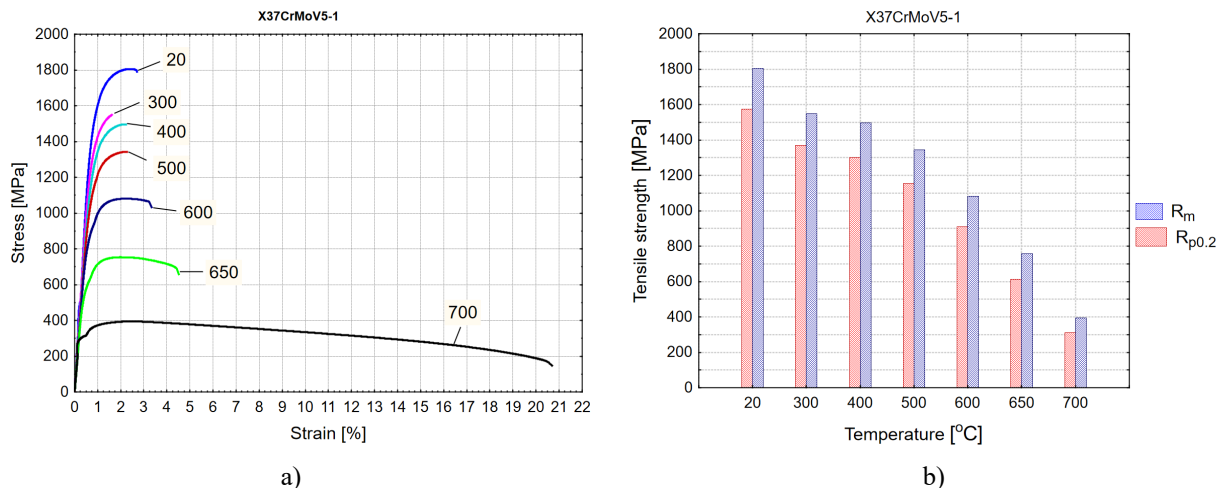


**Fig. 4** Stress-strain diagram (a) and histograms of obtained properties at elevated temperatures (b)

The testing of the H11 tool steel showed that a significant decrease in tensile strength occurs at the temperatures higher than 650 °C (Figure 4). In fact, the results show a quick reduction in the ultimate tensile strength as soon as 600 °C is exceeded, but the full collapse occurs at 650 °C and above. A similar tendency was discovered in the previous study on the influence of high temperatures on tensile strength of the structural steel S690QL [23], where it was concluded that a decrease in tensile properties occurs at 450 °C. The tensile strength decrease with a temperature increase is expected due to recrystallization and softening. Microstructure softening is a combined action of temperature and stress. In true service conditions, the material is submitted to the two effects, each of them showing a cyclic evolution. Creep and stress-rupture tests, which combine the consequences of temperature and stress, are the first step to roughly classify materials, even if the cyclic parameter is not present; time to rupture in a simple stress-rupture test may be approximately linked to creep deformation speed. Creep, and consequently stress relaxation, when the heated surface of the tool is closely maintained in contact with the material to be transformed, is not significant for 5% chromium steels for temperatures below 500 °C but must be taken into account for temperatures above that. Figures 6a and 6b show that the stress-rupture resistance of the tested steel is much better at 500-550 than at 600 °C [6]. With a further temperature increase this decrease is more evident.

It is important here to mention that in some cases due to temper embrittlement the strength is higher at higher tempering temperatures than at lower tempering temperatures. Temper embrittlement causes an increase in hardness and a decrease in the toughness of steel. Taking into account that an (independent) increase in hardness occurs simultaneously, this phenomenon is called the secondary hardness. The reason for the appearance of the temper embrittlement is caused by the presence of specific impurities in the steel, which segregate to prior austenite grain boundaries during heat treatment (mostly within 400-600 °C range). The main embrittling elements (in order of importance) are antimony, phosphorous, tin and arsenic. This was confirmed by some earlier research [24, 25]. That is one of the main reasons why after the reparatory welding tools have to be cooled faster for this temperature interval or to be careful to avoid tempering at given temperatures.

It should be noted that the presence of vanadium carbide particles in the martensite matrix also contributes to the high yield strength and, at the same time, increases the wear resistance [15]. The presence of such particles forms a part of the microstructure and may even precipitate at high cooling rates corresponding to oil quenching.

### 3.1 Strain hardening curves for H11 steel

Strain hardening of steel occurs during the tensile loading within the plasticity domain. This is why it is necessary to be familiar with the properties of the material within the plasticity domain, so that its stress and strain behaviour could be predicted. Due to big problems that arise during the experimental measurement of the main strains, a simpler form of the hardening curve is used as the functional dependence of the specific strain resistance and strain represented graphically. The material strain hardening curves are the initial point for the derivation of the FEM numerical analysis. There are several types of approximations; two of them are given here:

$$K = C \cdot \varphi^n, \tag{1}$$

where:  $C = R_m \frac{e^n}{n^n}$ ;

$C$  and  $n$  are the material constants, while  $\varphi = \ln(l/l_0)$  is the natural (logarithmic) strain.

The detailed procedure for the determination of the hardening curves is given in [23].

The hardening curve was calculated for a single specimen at each testing temperature and the obtained results are shown in Table 4 and Figure 6. That data was then used for the FE analysis. The curve that would be related to the temperature of 700 °C is not given due to the high deformation over 25 %.

**Table 4** Strain hardening curves for each specimen

Steel (AISI)	Sample No.	Testing temperature, °C	Strain hardening curves, $K=C\cdot\varphi^n$ , MPa
H11	1	20	$1961.3 \cdot \varphi^{0.01667}$
	2	300	$1606 \cdot \varphi^{0.0132}$
	3	400	$1453.5 \cdot \varphi^{0.01528}$
	4	500	$1496.3 \cdot \varphi^{0.01217}$
	5	600	$1173.4 \cdot \varphi^{0.01597}$
	6	650	$817.3 \cdot \varphi^{0.015}$
	7	700	$440 \cdot \varphi^{0.02176}$



**Fig. 5** Failure modes of H11 steel specimens at elevated temperatures

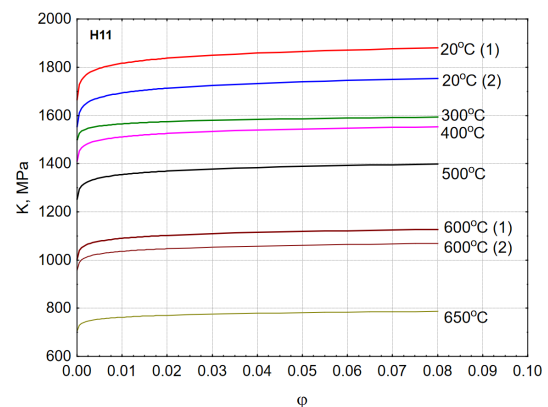


**Fig. 6** Strain hardening curves for each testing temperature

#### 4. FEM analysis of the tensile test

The second part of the paper presents the performed numerical analysis based on the finite element method and carried out using the PAK software [26]. The objective of the numerical analysis is to determine the degree of agreement between the results obtained experimentally and those obtained numerically. If the numerical simulation can reliably provide results that are similar to the experimental results at a satisfactory level, then expensive and long experiments of this type can be avoided in further research.

##### 4.1 Large strain elastic-plastic analysis

The stress integration algorithm for large strain deformations in the isotropic plasticity based on the multiplicative decomposition of the deformation gradient using the logarithmic strains is given in details in [23]. Due to the low plasticity and ultra-high strength of the tested steel it can be concluded that the visible necking is missing up to the temperatures of 650 °C.

##### 4.2 Numerical results

The specimen is modelled with 2,400 3D solid elements with 20 nodes per element. An elastic-plastic material model with isotropic hardening was used. The hardening zone is described by the Ramberg-Osgood equation:

$${}^t\sigma_y = \sigma_{y0} + C_y \left( {}^t\bar{\epsilon}^P \right)^n, \quad (2)$$

where  $\sigma_{y0}$  is the initial yield stress,  ${}^t\bar{\epsilon}^P$  the normalized effective plastic strain,  $C_y$  and  $n$  the material constants.

The obtained results for stress and logarithmic strain are compared with the experimental results. Figure 7 shows comparative diagrams within the temperature range from 20 to 700 °C. The obtained numerical results compared to the experimental results indicate that the deviation in stress is small but the deviation in strain is relatively large and not uniform, being the largest at 500 °C. One can consider restrictions of the model used in the numerical analysis to be the cause for these deviations since the model did not take all the variables in the tension process into account. The restriction of this model is also that the Ramberg-Osgood relationship can give results valid only up to the ultimate strength [27, 28], while strength hardening occurs, so there are no results for the zone after the ultimate strength is reached. Some further research should consider the use of more complex mathematical models such as the models shown in [29-31], which refer to the micromechanical analysis.

In addition, the effective stress and effective plastic strain are shown in Figs 8-14 for the moment before the fracture of the specimen occurs, at all testing temperatures. By analysing the deformed models tested at different temperatures one can notice that necking is visible at the temperatures greater than 600 °C, which is very similar to the real deformation that occurred on the experimentally tested specimens (Fig. 5).

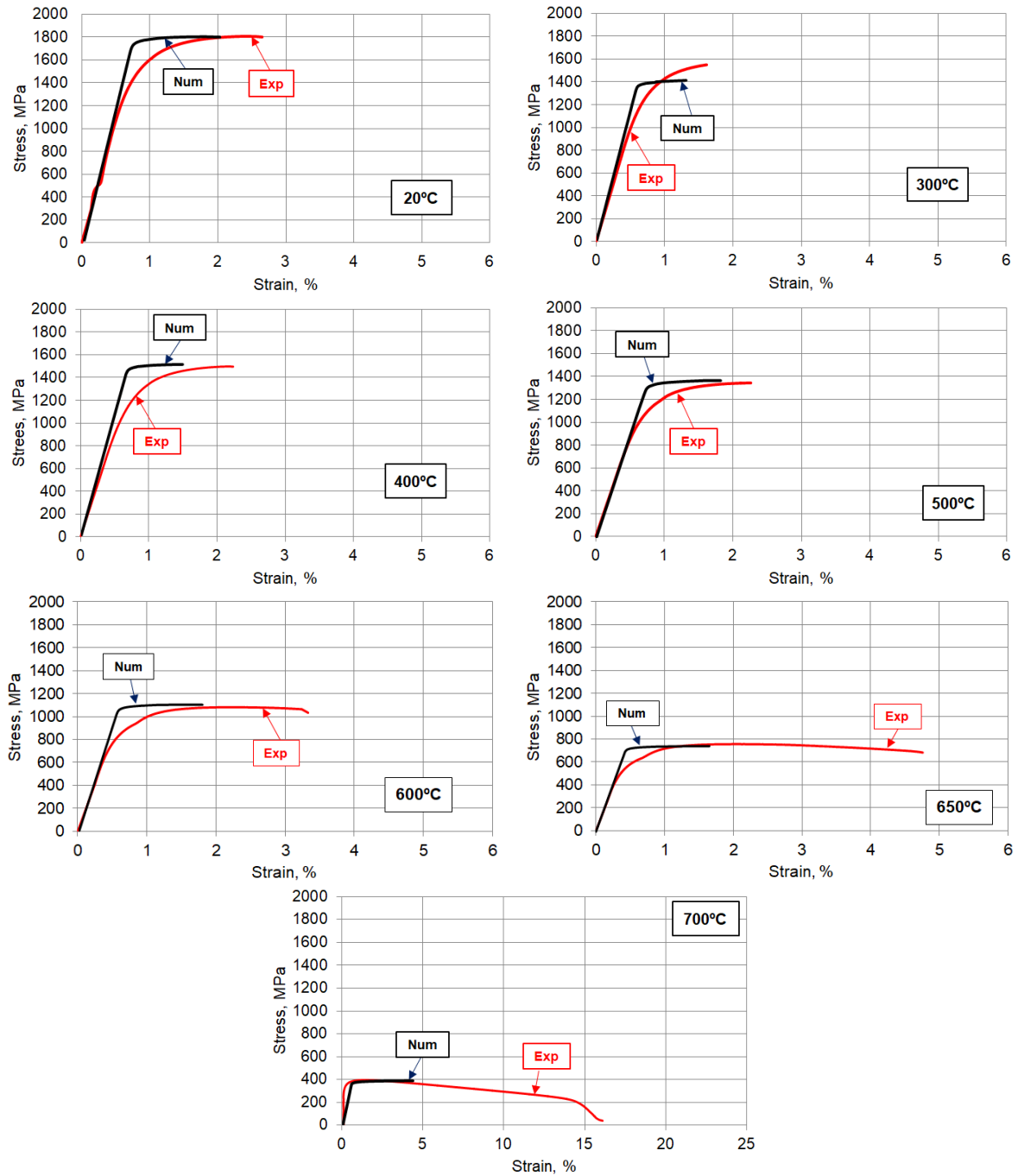


Fig. 7 Diagrams of experimental and numerical tensile testing in temperature range from 20 to 700°C

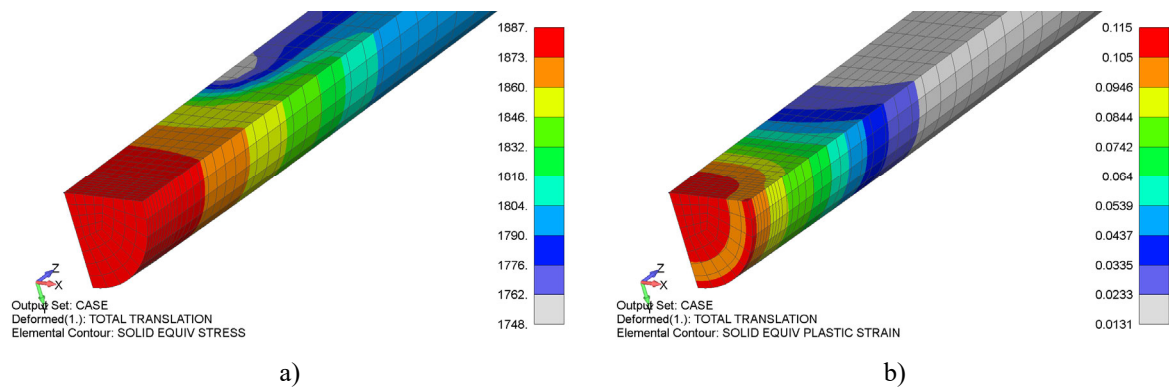


Fig. 8 Effective stress (a) and effective plastic strain (b) at the moment before fracture at 20 °C

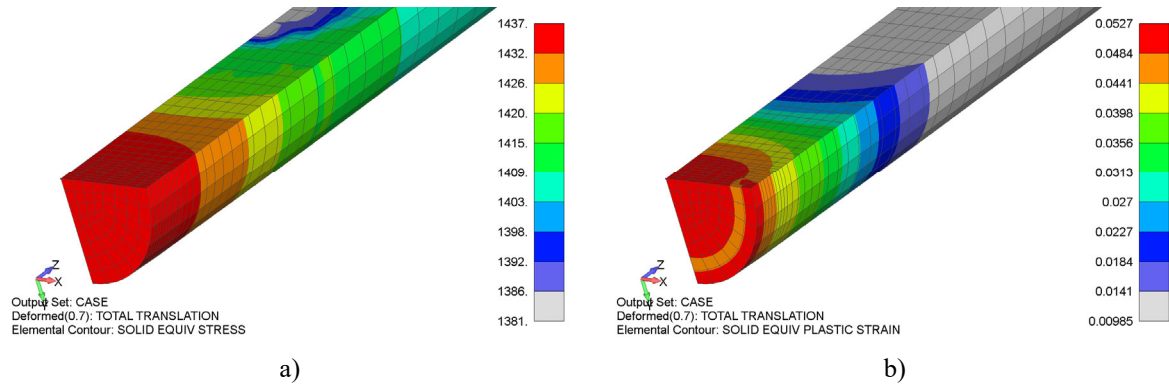


Fig. 9 Effective stress (a) and effective plastic strain (b) at the moment before fracture at 300 °C

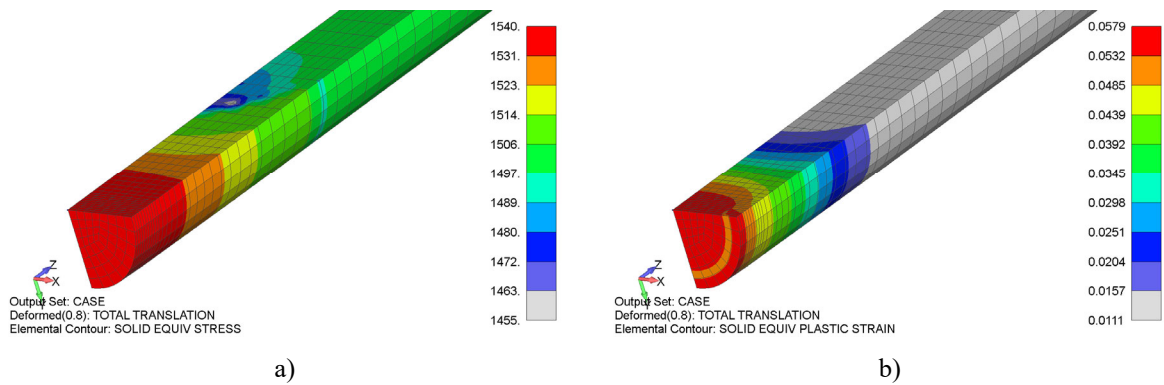


Fig. 10 Effective stress (a) and effective plastic strain (b) at the moment before fracture at 400 °C

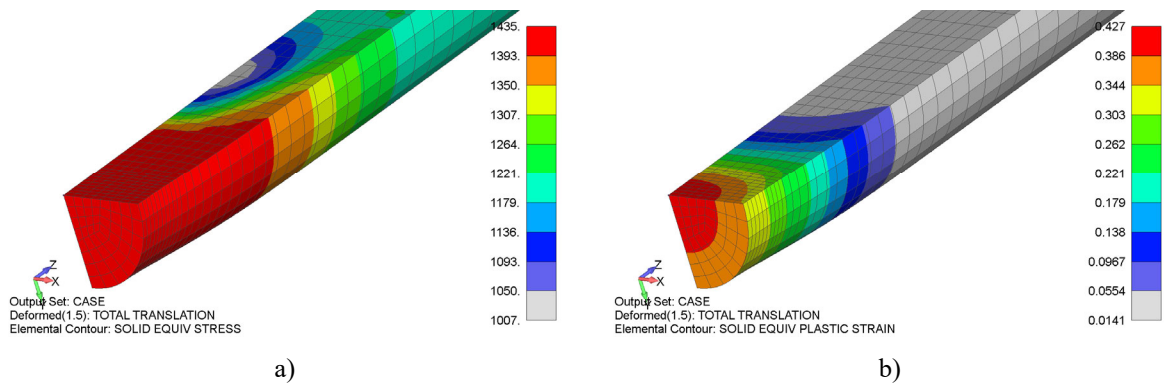


Fig. 11 Effective stress (a) and effective plastic strain (b) at the moment before fracture at 500 °C

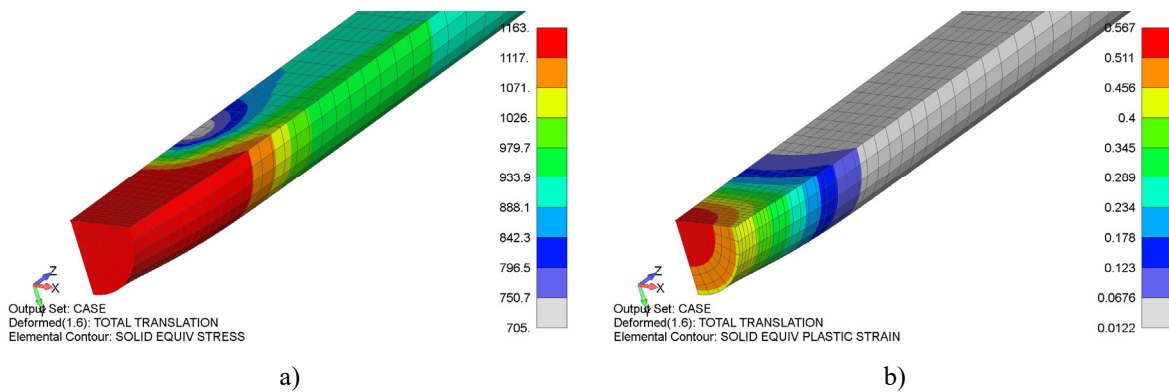
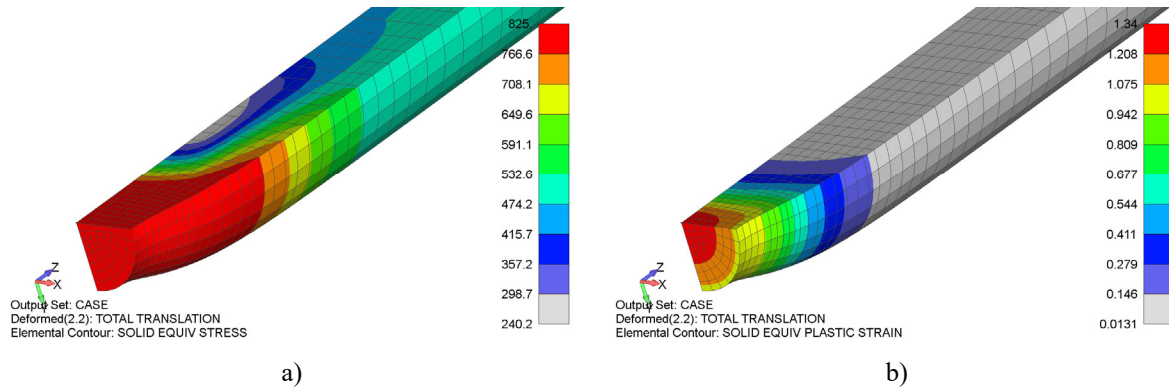
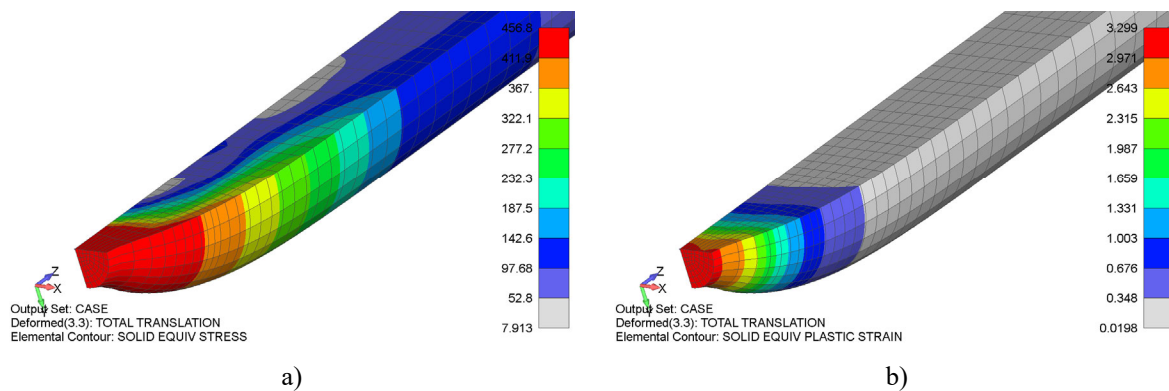


Fig. 12 Effective stress (a) and effective plastic strain (b) at the moment before fracture at 600 °C



**Fig. 13** Effective stress (a) and effective plastic strain (b) at the moment before fracture at 650 °C



**Fig. 14** Effective stress (a) and effective plastic strain (b) at the moment before fracture at 700 °C

## 5. Conclusion

The results obtained in this study show the influence of elevated temperatures on mechanical properties of the high quality hot work tool steel H11. The specimens were tested in the temperature range from 20 to 700 °C. The obtained experimental results show that this steel is very stable up to the temperatures of 500 °C to 550 °C and that a drop in mechanical properties occurs at the temperatures above 600 °C. At these temperatures a significant decrease in the yield stress and tensile strength of the specimens occurs. The elongation ability of this steel is relatively small and it does not change until about 600 °C, after which the application of this steel becomes senseless since its hardness becomes too low. The experiments confirm that the H11 steel behaves reliably up to the mentioned temperatures, so the conclusion is that it can safely be applied in the manufacture of forging dies, although they should be occasionally cooled by graphite suspensions and the surface temperature must be monitored and controlled, so that it would not surpass the critical temperature of 550 °C.

The developed numerical model can be considered as satisfactory since the obtained results are similar to the experimental results. The authors will conduct further research to try to improve the adopted model but it can be said that this model can be used for calculations when experiments cannot be carried out. The authors hope that the results presented in this paper will prove useful to engineers in building structures, parts and assemblies made of the steel H11.

## Acknowledgement

This research was partially financially supported by the Ministry of Education, Science and Technological Development of the Republic of Serbia within the project TR35024.

## REFERENCES

- [1] Arsić D, Lazić V, Samardžić I, Nikolić R, Aleksandrović S, Djordjević M, Hadzima B. Impact of the hard facing technology and the filler metal on tribological characteristics of the hard faced forging dies. *Tehnički vjesnik – Technical Gazette* 2015; 22(5): 1353-1358. <https://doi.org/10.17559/tv-20150408152638>
- [2] Arsić D, Lazić V, Sedmak A, Nikolić R, Aleksandrović S, Djordjević M, Bakić R. Selection of the optimal hard facing (HF) technology of damaged forging dies based on cooling time  $t_{8/5}$ . *Metallurgija - Metallurgy* 2016; 55(1): 103-106.
- [3] Lazić V, Sedmak A, Aleksandrović S, Milosavljević D, Čukić R, Grabulov V. Repairation of the damaged forging hammer mallet by hard facing and weld cladding, *Technical Gazette* 2009; 16(4): 107-113.
- [4] Lazić V, Sedmak A, Samardžić I, Aleksandrović S, Arsić D, Milosavljević D, Đorđević M. Shear strength testing of hardfaced samples using special tool on an universal testing machine. *Structural Integrity and Life* 2015; 15(1): 15-18.
- [5] Zouaghi A, Velay V, Soveja A, Pottier T, Cheikh M, Rezaï-Aria F. A multi-scale approach to investigate the nonlinear subsurface behavior and strain localization of X38CrMoV5-1 martensitic tool steel: Experiment and numerical analysis. *International Journal of Plasticity* 2016; 87: 130-153. <https://doi.org/10.1016/j.ijplas.2016.09.007>
- [6] Shah M, Mabru C, Rezaï-Aria F. Investigation of crack propagation in X38CrMoV5 (AISI H11) tool steel at elevated temperatures. *Procedia Engineering* 2010; 2: 2045-2054. <https://doi.org/10.1016/j.proeng.2010.03.220>
- [7] Shah M, Mabru C, Rezaï-Aria F. Characterisation of the surface damage of X38CrMoV5 (AISI H11) tool steel at room temperature and 600 °C. *Fatigue & Fracture of Engineering Materials & Structures* 2015; 38(6): 742-754. <https://doi.org/10.1111/ffe.12280>
- [8] Jiang QY, Zhao HY, Yang HF. Numerical simulation of the thermomechanical behavior of a hot stamping die. *Strength of Materials* 2018; 50(1): 124-129. <https://doi.org/10.1007/s11223-018-9950-4>
- [9] Qayyum F, Shah M, Shakeel O, Mukhtar F, Salem M, Rezaï-Aria F. Numerical simulation of thermal fatigue behavior in a cracked disc of AISI H-11 tool steel. *Engineering Failure Analysis* 2016; 62: 242-253. <https://doi.org/10.1016/j.engfailanal.2016.01.015>
- [10] Burja J, Tehovnik F, Godec M, Medved J, Podgornik B, Barbič R. Effect of electroslog remelting on the non-metallic inclusions in h11 tool steel. *Journal of Mining and Metallurgy Section B-Metallurgy* 2018; 54(1)B: 51-57. <https://doi.org/10.2298/jmmb160623053b>
- [11] Hawryluk M. Review of selected methods of increasing the life of forging tools in hot die forging processes. *Archives of Civil and Mechanical Engineering* 2016;16(4): 845-866. <https://doi.org/10.1016/j.acme.2016.06.001>
- [12] Gronostajski Z, Kaszuba M, Polak S, Zwierzchowski M, Niechajowicz A, Hawryluk M. The failure mechanisms of hot forging dies. *Materials Science & Engineering A* 2016; 657: 147-160. <https://doi.org/10.1016/j.msea.2016.01.030>
- [13] Fajoui J, Kchaou M, Sellami A, Branchu S, Elleuch R, Jacquemin F. Impact of residual stresses on mechanical behaviour of hot work steels. *Engineering Failure Analysis* 2018; 94: 33-40. <https://doi.org/10.1016/j.engfailanal.2018.07.020>
- [14] Reggiani B, Donati L, Zhou J, Tomesani L. The role of creep and fatigue in determining the high-temperature behaviour of AISI H11 tempered steel for aluminium extrusion die. *Journal of Materials Processing Technology* 2010; 210(12): 1613-1623. <https://doi.org/10.1016/j.jmatprotec.2010.05.009>
- [15] Grüning A, Lebsanft M, Scholtes B. Cyclic stress-strain behavior and damage of tool steel AISI H11 under isothermal and thermal fatigue conditions. *Materials Science and Engineering A*: 2010; 527: 1979-1985. <https://doi.org/10.1016/j.msea.2009.11.031>
- [16] Pastor A, Valles P, More W, Medina SF. Toughness improvement of steel X38CrMoV5-1 via alternative manufacturing process and prevention of catastrophic failure in safety parts. *Engineering Failure Analysis* 2017; 82: 791-801. <https://doi.org/10.1016/j.engfailanal.2017.07.025>
- [17] Šolić S, Podgornik B, Leskovšek V. The occurrence of quenching cracks in high-carbon tool steel depending on the austenitizing temperature. *Engineering Failure Analysis* 2018; 92: 140-148. <https://doi.org/10.1016/j.engfailanal.2018.05.008>
- [18] Leskovšek V, Šuštaršič B, Jutriša G. The influence of austenitizing and tempering temperature on the hardness and fracture toughness of hot-worked H11 tool steel. *Journal of Materials Processing Technology* 2006; 178: 328-334. <https://doi.org/10.1016/j.jmatprotec.2006.04.016>

- [19] Technical card of steels, Group LUCEFIN Lovin Steel, Lucefin S.p.A., Italy.
- [20] Tekauit İ, Demir H, Şeker U. Experimental analysis and theoretical modelling of cutting parameters in the drilling of AISI H13 steel with coated and uncoated drills. *Transactions of FAMENA* 2018; 42(2): 83-96. <https://doi.org/10.21278/tof.42207>
- [21] Saini N, Pandey C, Mahapatra MM, Mulik RS. On study of effect of varying tempering temperature and notch geometry on fracture surface morphology of P911 (9Cr-1Mo-1W-V-Nb) steel. *Engineering Failure Analysis* 2018; 85: 104-115. <https://doi.org/10.1016/j.engfailanal.2017.12.013>
- [22] ISO 6892-2:2011: Metallic materials - Tensile testing - Part 2: Method of test at elevated temperatures.
- [23] Arsić D, Djordjević M, Živković J, Sedmak A, Aleksandrović S, Lazić V, Rakić D. Experimental-numerical study of tensile strength of the high-strength steel S690QL at elevated temperatures. *Strength of Materials* 2016; 48(5): 687-695. <https://doi.org/10.1007/s11223-016-9812-x>
- [24] Grellier A, Siaux M. A new hot work tool steel for high temperature and high stress service conditions. *Proceedings of the 6th international tooling conference - The Use of Tool Steels: Experience and Research*, Karlstad University Sweden, 2002; 33-42.
- [25] Mutavdžić M, Lazić V, Milosavljević D, Aleksandrović S, Nikolić R, Čukić R, Bogdanović G. Determination of the optimal tempering temperature in hard facing of the forging dies. *Materials Engineering - Materialove inženierstvo* 2012; 19: 95-103.
- [26] Kojić M, et al. "PAK-S: Program for FE Structural Analysis", Faculty of Mechanical Engineering, University of Kragujevac, Kragujevac, Serbia, 1999.
- [27] Kamaya M. Ramberg-Osgood type stress-strain curve estimation using yield and ultimate strengths for failure assessments. *International Journal of Pressure Vessels and Piping* 2016; 137: 1-12. <https://doi.org/10.1016/j.ijpvp.2015.04.001>
- [28] Kolitsch S, Gänser HP, Pippan R. Dependence of fracture strain on flaw size in rail switches-Experiments and theoretical modelling. *Engineering Failure Analysis* 2018; 85: 50-61. <https://doi.org/10.1016/j.engfailanal.2017.12.010>
- [29] Younise B, Rakin M, Gubelj N, Medjo B, Sedmak A. Numerical simulation of constraint effect on fracture initiation in welded specimens using a local damage model, *Structural Integrity and Life* 2011; 11(1): 51-56.
- [30] Younise B, Sedmak A. Micromechanical study of ductile fracture initiation and propagation on welded tensile specimen with a surface pre-crack in weld metal. *Structural Integrity and Life* 2014; 14(3): 185-191.
- [31] Sedmak A. Computational fracture mechanics: An overview from early efforts to recent achievements, *Fatigue and Fracture of Engineering Materials and Structures* 2018; 41: 2438-2474. <https://doi.org/10.1111/ffe.12912>

Submitted: 30.05.2019

Accepted: 11.12.2019

Dušan Arsić  
Vukić Lazić  
Srbislav Aleksandrović  
Jelena Živković  
Faculty of Engineering, University of  
Kragujevac, Sestre Janjić 6, 34000  
Kragujevac, Serbia  
Aleksandar Sedmak  
Goran Mladenović  
Faculty of Mechanical Engineering,  
University of Belgrade, Kraljice Marije 16,  
11000 Belgrade, Serbia  
Milan Djordjević  
Faculty of Technical Sciences, University  
of Priština, Kneza Miloša 7, 38220  
Kosovska Mitrovica, Serbia  
Corresponding author: [dusan.arsic@fink.rs](mailto:dusan.arsic@fink.rs)